

Optical probing of the Coulomb interactions of an electrically pumped polariton condensate

M. Klaas,^{1, a)} S. Mandal,² T.C.H. Liew,² M. Amthor,^{3,4} S. Klemmt,^{3,4} L. Worschech,^{3,4} C. Schneider,^{3,4} and S. Höfling^{3,4}

¹⁾ *Technische Physik, Wilhelm-Conrad-Röntgen-Research Center for Complex Material Systems, Universität Würzburg, Am Hubland, D-97074 Würzburg, Germany*

²⁾ *Division of Physics and Applied Physics, School of Physical and Mathematical Sciences, Nanyang Technological University, Singapore 637371, Singapore*

³⁾ *Technische Physik, Wilhelm-Conrad-Röntgen-Research Center for Complex Material Systems, Universität Würzburg, Am Hubland, D-97074 Würzburg, Germany*

⁴⁾ *SUPA, School of Physics and Astronomy, University of St Andrews, St Andrews KY16 9SS, United Kingdom*

(Dated: 31 March 2017)

We report on optical probing of the Coulomb interactions in an electrically driven exciton-polariton laser. By positioning a weak non-resonant Gaussian continuous wave-beam with a diameter of $2\ \mu\text{m}$ inside an electrical condensate excited in a $20\ \mu\text{m}$ diameter micropillar, we study a repulsion effect which is characteristic of the part-excitonic nature of the microcavity system in strong coupling. It manifests itself in a modified real space distribution of the emission pattern. Furthermore, polariton repulsion results in a continuous blueshift of the emission with increased power of the probe beam. A Gross-Pitaevskii equation approach based on modeling the electrical and optical potentials explains our experimental data.

Exciton-polaritons can be created in quantum well microcavity structures as a result of the strong coupling of excitons and photons^{1,2}. Their bosonic nature allows the creation of a condensate^{3,4}, which is inherently non-equilibrium due to the dissipative character of the system. Advantageous for the formation of this quantum degenerate state is the small effective mass of the quasi-particles which allows condensation up to room temperature in wide bandgap semiconductors like ZnO⁵, GaN⁶ and organic materials^{7,8}. This macroscopically occupied state can show a variety of exciting many-body effects⁹. One of the most interesting, from an application viewpoint, is laser-like emission without the necessity for inversion, already proposed in 1996¹⁰. An advantage of such polariton light sources is the possibility for very low thresholds¹¹. Furthermore, adding the fact that they can exhibit up to shot-noise limited temporal coherence^{12,13} and considerable spatial coherence^{3,14}, the polariton laser is a promising future device for coherent ultra low power consumption applications.

Only recently polariton lasing under electrical pumping has been achieved^{15,16}. The Coulomb interactions emerging inside such a condensate are poorly understood, compared to optically driven condensates in planar samples^{17,18} and micropillars¹⁹. The interaction constants in purely optically driven condensates have been under intense research with values ranging from $2\text{-}50\ \mu\text{eV} * \mu\text{m}$ ²¹⁹⁻²²², most likely depending on different sample purities and excitation methods. The exact interactive nature of the polariton therefore remains on open topic. In optical experiments, the manipulation of the matter part of the condensate has been successfully used to achieve application relevant effects²³⁻²⁵, since the large

nonlinearity of the polariton system enables energy efficient switching processes, in comparison to traditional VCSEL devices. Therefore, a precise understanding of these interactions inherited from the excitonic part of the polariton is a necessary step for future electrically pumped device designs and is of interest to understand the fundamental interactive nature of the electrically formed condensates.

In this experiment, we place a weak spectrally far off non-resonant continuous wave optical excitation at different positions inside the electrically pumped polariton emission resolved in real space. This allows us to manipulate the potential energy landscape seen by the electrically excited polaritons and enables the observation of repulsion effects. This repulsion results in changes in the spatial distribution of the polariton emission. The investigated sample is comparable to the one in ref.¹⁵ and consists of 23(27) doped AlAs/GaAs distributed Bragg reflectors (DBRs) in the bottom and top mirrors respectively. The carbon doping of the top mirror allows the injection of holes, while the silicon doped bottom DBR structure facilitates electron injection. The Fabry-Perot type cavity spacer is a λ cavity and contains four InGaAs quantum wells (QWs) placed at the antinodes of the electrical field inside the structure. The injected holes and electrons then form excitons in the QWs. Figure 1a) shows a sketch of our device and the experiment. We have etched pillars with a diameter of $20\ \mu\text{m}$ in the microcavity which realizes a photonic potential and a more localized current injection. After the etching the sample was planarized by a polymer (benzocyclobutene (BBC)). The current injection is realized by the ring shaped gold contacts on the micropillar, which also leave a $10\ \mu\text{m}$ diameter aperture for optical investigation and decay of the polaritons out of the microcavity. The gold contacts were defined by lithography and evaporated on top of the

^{a)} martin.klaas@physik.uni-wuerzburg.de

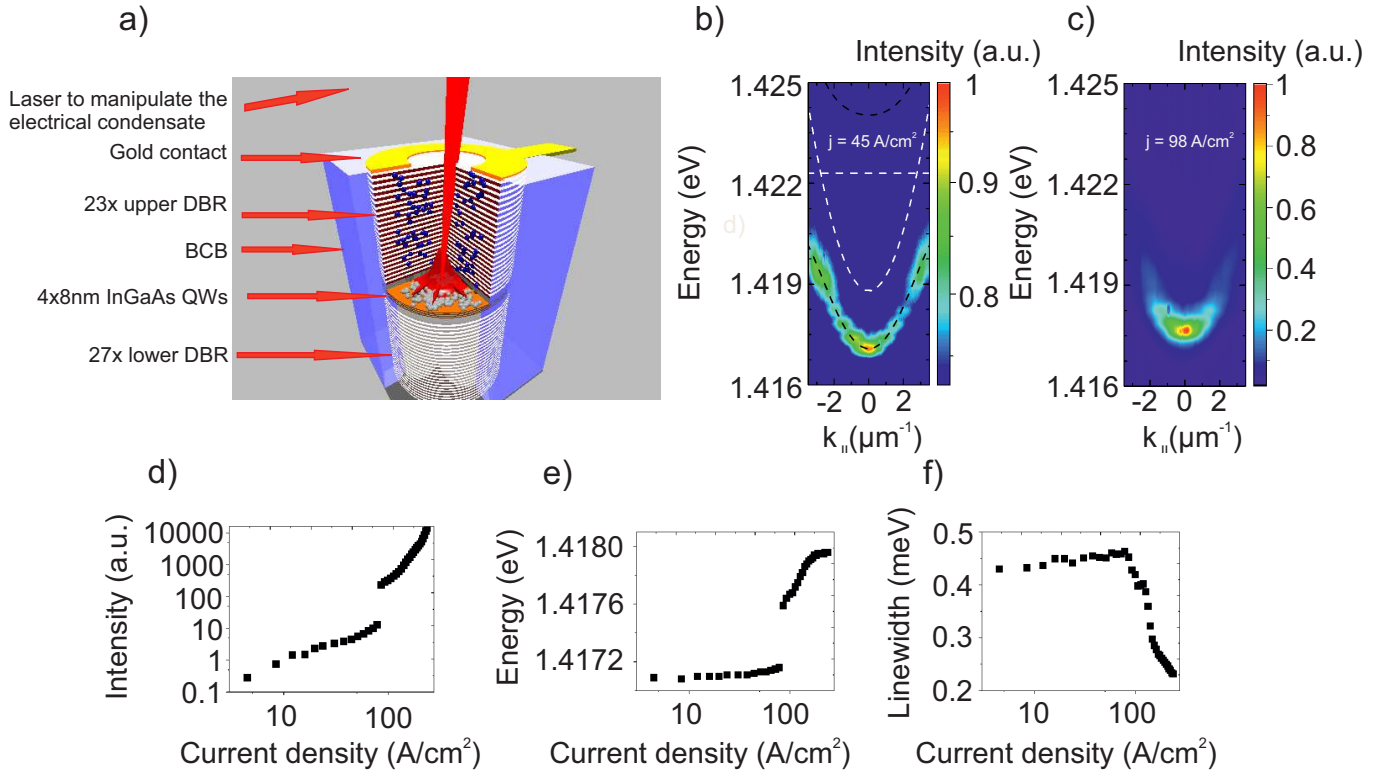


FIG. 1. a) Sketch of the electrically driven polariton laser and a scheme of the experiment, in which a laser beam produces a repulsion effect in the polariton emission. b) Dispersion relation of the polariton emission at an electrical injection of $j=45$ A/cm², the dashed white lines show the exciton and cavity mode, while the black dashed lines shows the theoretical dispersions of the lower and upper polariton branch. c) Dispersion in the condensate regime with a current of $j=98$ A/cm². d)/e)/f) Input-output characteristic of the device showing intensity/blueshift/linewidth of the condensate emission determined by a Lorentz fit from the integrated emission at $k=0 \pm 0.1 \mu\text{m}^{-1}$.

micropillar devices.

All our experiments have been performed at 5 T. The magnetic field improves light-matter coupling due to an increased Rabi-splitting²⁶ and has beneficial effects on the relaxation towards the groundstate¹⁵. The temperature was set to 5 K in a liquid helium cooled magnetocryostat. This low temperature increases the stability of the excitons. The Q-factor was estimated from a low power measurement at far red detuning of the sample to be ~ 6000 , which enables polariton condensation due to the high photon lifetime which is necessary for the relaxation process. The Rabi-splitting of the sample is 5.5 meV (6 meV at 5 T), which was determined by reflection measurements. The detuning of the investigated pillar sample was -3.5 meV at 5 T, which corresponds to a fraction of 25 % exciton and 75 % photon.

The angle resolved electroluminescence spectrum can be seen in figure 1b) and c), below and above threshold respectively. To obtain these measurements, we used a standard Fourier space setup²⁷. The upper polariton branch is not visible due to depletion resulting from fast relaxation^{28,29}. The linear regime below threshold shows the characteristic discretized mode spectrum due to photonic confinement realized by the micropillar structure. At high current densities, when the lasing threshold is

reached, stimulated scattering sets in and the polaritons occupy a macroscopically populated groundstate, defined by the micropillar trap. A weak emission of higher modes is also observed, such a coexistence of polariton condensates is a frequently observed phenomenon in open dissipative systems.^{19,27} Figures 1d), e) and f) show the input-output characteristics. These were obtained by integrating the emission around $k=0 \pm 0.1 \mu\text{m}^{-1}$ and applying a Lorentzian lineshape fit for different applied currents. We observe a nonlinearity in intensity output, a continued blueshift and a drop of the linewidth above threshold at $j=72$ A/cm². This nonlinearity in intensity marks the lasing threshold and the continued blueshift above threshold is a sign of increased exciton-exciton interactions³⁰, typical for a polariton condensate. The energy gap at the threshold stems from the intrinsic bistability of our system³¹. Below threshold this blueshift is linear and after condensation it obtains a logarithmic shape as previously observed in³². At $j=200$ A/cm² a second threshold shows the system transitioning into photon lasing.

In the experiment, the incoherent electrical pump from the ring contact creates an almost rotational symmetric condensate inside the micropillar structure in real space as seen in figure 2a). The low fraction of

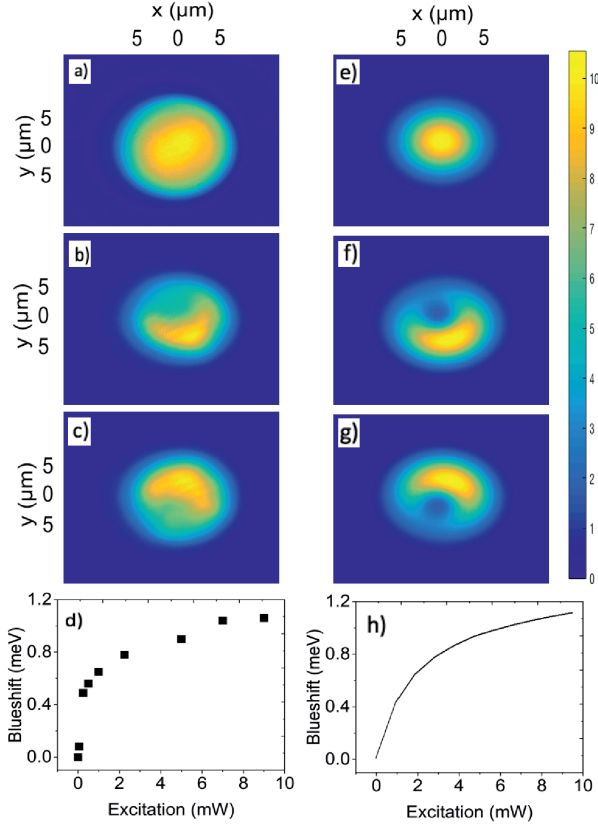


FIG. 2. a) Real space image of the polariton condensate emission at an injection current of $j = 100 \text{ A/cm}^2$. b) The condensate with the same injection current, this time with an additional optical Gaussian beam (658 nm, 5 mW) and an edge pass filter for the laser. c) The real space position of the beam is varied such that the condensate is repelled into the other direction. d) Blueshift behavior with increased laser excitation power. Theoretical ground state profiles from Eq. 1 without e) and with f), g) an additional laser drive. h) Power dependence of the ground state energy shift. Parameters: $m_{\text{eff}} = 8.33 \times 10^{-6}$ of the free electron mass, $g_R = 45.95$, $P_{\text{peak}} = 1.3 \text{ meV}$, $\Gamma = 0.13 \text{ meV}$. The additional excitation beam was positioned at $(-0.2, 0.5) / (-0.2, -0.5) \mu\text{m}$ and had a strength of 18 meV for (f) and (g).

higher polariton modes, which amount to approximately 2 % of the overall emission intensity, yields a slightly non Gaussian real space emission shape. Figure 2b) and c) show cases when we add an additional optical beam (at 658 nm, 5 mW, highpass filter with a cut off at 750 nm) inside the condensate. The beam diameter is approximately $2 \mu\text{m}$, focused by an objective with $f = 10 \text{ mm}$ and $\text{NA} = 0.4$. At the spot of the optical excitation the condensate is repelled, because the optical pump creates an additional exciton- and a low density polariton reservoir. This effect can be induced at any position off center to move the condensate emission at will to the edge of the ring structure. It is important to notice that polariton condensation with only the optical

excitation at 658 nm could not be observed. Furthermore, above the photon lasing threshold, no repulsion effects are observed. The repulsion is accompanied by a continuous blueshift of the emission in fig. 2d). Increasing the excitation power of the laser results in repulsive interactions of the electrically driven polaritons with the additional particles.

The theoretical description of exciton-polariton condensates in real space is often made by applying a driven-dissipative mean-field Gross-Pitaevskii-type equation^{33,34}. While such an equation represents a non-Hermitian system, it can still be subjected to a modal analysis, solving the linearized equations as a time-independent Schrödinger equation³⁵:

$$E_n \psi_n(\mathbf{x}) = \left(-\frac{\hbar^2 \nabla^2}{2m_{\text{eff}}} + \left(g_R + \frac{i}{2} \right) P(\mathbf{x}) - \frac{i\Gamma}{2} \right) \psi_n(\mathbf{x}) \quad (1)$$

Here $\psi_n(\mathbf{x})$ are non-Hermitian modes with energies E_n . m_{eff} is the polariton effective mass. $P(\mathbf{x}) = P_e(\mathbf{x}) + P_l(\mathbf{x})$ is the pumping strength, being composed of a ring shaped electrical driving $P_e(\mathbf{x})$ and a Gaussian shaped laser driving $P_l(\mathbf{x})$. g_R describes the repulsive interactions between a reservoir of exciton states created by the driving and polaritons. For simplicity, these are assumed stronger than the interactions between polaritons themselves. Γ is the polariton decay rate.

The ground-state wavefunctions obtained from Eq. 1 are shown in Figs. 2e) and 2f), in the cases without and with the additional laser excitation. These demonstrate the optically induced repulsion of the experiment, consistent with the condensation of polaritons in the ground state. Figure 2g) illustrates that the repulsion effect can also be induced at another position. The theoretically calculated dependence of the ground state energy on the optical excitation power (Fig. 2h)) has a sublinear dependence, which is expected due to reduced overlap of repelled wavefunctions with the increasing optically-induced potential.

In conclusion, we have demonstrated the possibility to probe the Coulomb interactions and the quantum fluid nature of the electrically driven polariton condensate by an additional optically induced potential. The observed repulsion effects can be theoretically described by superposition of a Gaussian potential and the ring shaped electrical pump. This opens up the possibility to further manipulate the electrical condensate with additional optical external potentials to achieve control over the polariton flow for electrical polariton logic elements.

ACKNOWLEDGMENTS

The authors would like to thank the State of Bavaria for financial support. We thank M. Lerner and A. Wolf for support in sample fabrication. SM and TL were supported by the NAP Start-Up grant M4081630 and MOE

REFERENCES

- ¹C. Weisbuch, M. Nishioka, A. Ishikawa, and Y. Arakawa, *Phys. Rev. Lett.* **69**, 3314 (1992).
- ²A. Kavokin, J. Baumberg, G. Malpuech, and F. Laussy, *Microcavities* (Clarendon, Oxford, U.K., 2006).
- ³J. Kasprzak, M. Richard, S. Kundermann, A. Baas, P. Jeambrun, J. M. J. Keeling, F. M. Marchetti, M. H. Szymanska, R. Andre, J. L. Staehli, V. Savona, P. B. Littlewood, B. Deveaud, and L. S. Dang, *Nature* **443**, 409 (2006).
- ⁴R. Balili, V. Hartwell, D. Snoko, L. Pfeiffer, and K. West, *Science* **316**, 1007 (2007).
- ⁵T. Lu, Y. Lai, Y. Lan, S. Huang, J. Chen, Y. Wu, W. Hsieh, and H. Deng, *Opt. Express* **20**, 5530 (2012).
- ⁶G. Christmann, R. Butte, E. Feltn, J. Carlin and N. Grandjean, *Appl. Phys. Lett* **93**, 051102 2008.
- ⁷J. D. Plumhof, T. Stoferle, L. Mai, U. Scherf, and R. F. Mahrt, *Nat. Mat.* **13**, 247 (2014).
- ⁸K. S. Daskalakis, S. A. Maier, R. Murray, and S. Kena-Cohen, *Nat. Mat.* **13**, 271 (2014).
- ⁹I. Carusotto, and C. Ciuti, *Rev. Mod. Phys.* **85**, 299 (2013).
- ¹⁰A. Imamoglu, R. J. Ram, S. Pau, and Y. Yamamoto, *Phys. Rev. A* **53**, 4250 (1996).
- ¹¹H. Deng, G. Weihs, D. Snoko, J. Bloch, and Y. Yamamoto, *PNAS* **100**, 15318 (2003).
- ¹²S. Kim, B. Zhang, Z. Wang, J. Fischer, S. Brodbeck, M. Kamp, C. Schneider, S. Hoefling and H. Deng, *Phys. Rev. X* **6**, 011026 (2016).
- ¹³A. P. D. Love, D. N. Krizhanovskii, D. M. Whittaker, R. Bouchekioua, D. Sanvitto, S. Al Rizeiqi, R. Bradley, M. S. Skolnick, P. R. Eastham, R. Andre and L. S. Dang, *Phys. Rev. Lett.* **101**, 067404 (2008).
- ¹⁴H. Deng, G. Solomon, R. Hey, K. H. Ploog, and Y. Yamamoto, *Phys. Rev. Lett.* **99**, 126403 (2007).
- ¹⁵C. Schneider, A. Rahimi-Iman, N. Y. Kim, J. Fischer, I.G. Savenko, M. Amthor, M. Lermer, A. Wolf, L. Worschech, V. D. Kulakovskii, I. A. Shelykh, M. Kamp, S. Reitzenstein, A. Forchel, Y. Yamamoto, and S. Hoefling, *Nature* **497**, 348 (2013).
- ¹⁶P. Bhattacharya, B. Xiao, A. Das, S. Bhowmick, and J. Heo, *Phys. Rev. Lett.* **110**, 206403 (2013).
- ¹⁷E. Wertz, L. Ferrier, D. D. Solnyshkov, R. Johne, D. Sanvitto, A. Lemaitre, I. Sagnes, R. Grousson, A. V. Kavokin, P. Senellart, G. Malpuech, and J. Bloch, *Nat. Phys.* **6**, 860 (2010).
- ¹⁸G. Tosi, G. Christmann, N. G. Berloff, P. Tsotsis, T. Gao, Z. Hatzopoulos, P. G. Savvidis, and J. J. Baumberg, *Nat. Phys.* **8**, 190 (2012).
- ¹⁹L. Ferrier, E. Wertz, J. Johne, D. Solnyshkov, P. Senellart, I. Sagnes, A. Lemaitre, G. Malpuech, and J. Bloch, *Phys. Rev. Lett.* **106**, 126401 (2011).
- ²⁰A. S. Brichkin, S. I. Novikov, A. V. Larionov, V. D. Kulakovskii, M. M. Glazov, C. Schneider, S. Hoefling, M. Kamp, and A. Forchel, *Phys. Rev. B* **84**, 195301 (2011).
- ²¹P. M. Walker, L. Tinkler, D. V. Skryabin, A. Yulin, B. Royall, I. Farrer, D. A. Ritchie, M. S. Skolnick, and D. N. Krizhanovskii, *Nat. Comm.* **6**, 8317 (2015).
- ²²S. R. K. Rodriguez, A. Amo, I. Sagnes, L. Le Gratiet, E. Galopin, A. Lemaitre, and J. Bloch, *Nat. Comm.* **7**, 11887 (2016).
- ²³T. Gao, P. S. Eldridge, T. C. H. Liew, S. I. Tsintzos, G. Stavrinidis, G. Deligeorgis, Z. Hatzopoulos, and P. G. Savvidis, *Phys. Rev. B* **85**, 235102 (2012).
- ²⁴D. Ballarini, M. de Giorgi, E. Cancellieri, R. Houdre, E. Giacobino, R. Cingolani, A. Bramati, G. Gigli, and D. Sanvitto, *Nat. Comm.* **4**, 1778 (2013).
- ²⁵H. S. Nguyen, D. Vishnevsky, C. Sturm, D. Tanese, D. Solnyshkov, E. Galopin, A. Lemaitre, I. Sagnes, A. Amo, G. Malpuech, and J. Bloch, *Phys. Rev. Lett.* **110**, 236601 (2013).
- ²⁶B. Pietka, D. Zygmunt, M. Krol, M. R. Molas, A. A. L. Nicolet, F. Morier-Genoud, J. Szczytko, J. Lusakowski, P. Zieba, I. Tralle, P. Stepnicki, M. Matuszewski, M. Potemski, and B. Deveaud, *Phys. Rev. B* **91**, 075309 (2015).
- ²⁷C. W. Lai, N. Y. Kim, S. Utsunomiya, G. Roumpos, H. Deng, M. D. Fraser, T. Byrnes, P. Recher, N. Kumada, T. Fujisawa, and Y. Yamamoto, *Nature* **450**, 529 (2007).
- ²⁸E. Wertz, L. Ferrier, D. Solnyshkov, P. Senellart, D. Bajoni, A. Miard, A. Lemaitre, G. Malpuech, and J. Bloch, *Appl. Phys. Lett.* **95**, 051108 (2009).
- ²⁹V. D. Kulakovskii, A. V. Larionov, S. I. Novikov, S. Hoefling, C. Schneider, and A. Forchel, *JETP Lett.* **92**, 595 (2010).
- ³⁰C. Ciuti, V. Savona, C. Piermarocchi, A. Quattropani, and P. Schwendimann, *Phys. Rev. B* **58**, 7926 (1998).
- ³¹M. Amthor, T. C. H. Liew, C. Metzger, S. Brodbeck, L. Worschech, M. Kamp, I. A. Shelykh, A. V. Kavokin, C. Schneider, and S. Hoefling, *Phys. Rev. B* **91**, 081404 (2015).
- ³²G. Roumpos, W. Nitsche, S. Hoefling, A. Forchel, and Y. Yamamoto, *Phys. Rev. Lett.* **104**, 126403 (2010).
- ³³M. Wouters, and I. Carusotto, *Phys. Rev. Lett.* **99**, 140402 (2007).
- ³⁴J. Keeling, and N. G. Berloff, *Phys. Rev. Lett.* **100**, 250401 (2008).
- ³⁵S. Khan, and H. E. Türeci, *Phys. Rev. A* **94**, 053856 (2016).